

# Model Companion 3.0

*A Short User Manual for a Model of Reverberation Chamber Based on Image Theory*

Emmanuel Amador, Philippe Besnier, Christophe Lemoine  
emmanuel.amador@insa-rennes.fr

October 18, 2011





*But though all our knowledge begins with experience,  
it does not follow that it all arises out of experience.*

Immanuel Kant

*A boat's a boat, but the mystery box could be anything. It could even be a boat.*

Peter Griffin



# Contents

<b>Foreword</b>	<b>7</b>
<b>Licensing</b>	<b>8</b>
<b>Content of the Archive</b>	<b>10</b>
<b>Release Notes</b>	<b>11</b>
<b>1 Understanding the Model</b>	<b>13</b>
1.1 Image Theory . . . . .	13
1.2 Image Theory Applied to Cavities . . . . .	14
<b>2 Image Creator</b>	<b>18</b>
2.1 Usage . . . . .	18
2.2 How to Construct Images When Time is Money . . . . .	18
<b>3 CIR Calculation and More</b>	<b>20</b>
3.1 CIR Computation . . . . .	20
3.2 Frequency Response and Response to an Arbitrary Waveform . . . . .	20
<b>4 Stirring Process</b>	<b>23</b>
4.1 Source Stirring . . . . .	23
4.2 Paddle Simulation . . . . .	23
<b>5 Frequency domain direct calculation</b>	<b>24</b>
<b>6 Memory Usage</b>	<b>25</b>
<b>7 Loss Coefficient Estimation</b>	<b>26</b>
7.1 Measurement approach . . . . .	26



# Foreword

When we started the development of this model, we wanted to have a simple code that would allow to understand the behavior of a reverberation chamber in the pulse regime. We did not imagine that a model that simple, would carry the physics of a reverberation chamber. The model we have developed is able to describe both the time domain and the frequency domain and can be helpful to understand the physics beyond a reverberation chamber.

Thank you for using the model we developed. This model based on the image theory can simulate high quality factor rectangular cavities. Even if this model is relatively straightforward, this document can be helpful to have an overview of its possibilities. This document may change in the future. Critics, comments and suggestions are welcomed.

The Authors.

# Licensing

This model represents more than one year of work. The set of programs is provided under a license or a nondisclosure agreement, and it may be used only in accordance with terms of those agreements. No part of this documentation may be duplicated or distributed without the written permission of the authors. By using this software, you agree to credit the authors: Emmanuel Amador, Philippe Besnier and Christophe Lemoine from the Institut d'Électronique et de Télécommunications de Rennes (IETR) and the main article describing this model [1]. You can use the source-code and make modifications to suit your needs. You cannot distribute this software or an altered version of this software.



# Acknowledgements

This work is supported by the French ministry of defence DGA (Direction Générale de l'Armement) with a Ph.D grant.

# Content of the Archive

Included in the Zip file are this document and four Matlab/Octave programs:

- `ImageCreator.m` is a program that generates the sources.
- `CIR.m` is a function that calculates the channel impulse response for a given position.
- `CIR8th.m` is a subfunction used by `CIR.m`.
- `ExampleTD.m` is a sample program that uses the `CIR.m` function. It returns the channel impulse response, the frequency response (computed with a FFT) and the response for a chosen signal at a given reception point in the cavity.
- `FR.m` is a function that calculates the frequency response for a given position.
- `FR8th.m` is a subfunction used by `FR.m`.
- `ExampleFD.m` is a sample program that uses the `FR.m` function. It returns the frequency response of the chamber at a given reception in the cavity. The frequency response allows to use introduce frequency dependent losses in the model.
- `Image_Theory_Model_Full_losses.zip` contains a more complex loss simulation, uses a little more memory. Use this version of the program only if you need a different loss coefficient for each axis. Please note that the `ImageCreator_full.m` script is not completely optimized and computation may be a little longer than with `ImageCreator.m`, we may update the script in the next version.

# Release Notes

- v 3.0 - October 2011, introduction of a new harmonic computation of the frequency response. The loss coefficient can be a function of the frequency. We can also add volumetric absorption by water in the air.
- v 2.0 - November 2009, Image Creation redesigned, in comparison with v 1.0, the memory usage is divided by 64. All the other programs are deeply modified to use the new image sources matrixes. The lite version of the model becomes the standard version and the previous standard version becomes the full losses version, that uses more memory.
- v 1.3 - October 2009, ImageCreator improved, uses far less memory
- v 1.2 - December 2009, Lite versions of the programs.
- v 1.1 - November 2009, CIR function added.
- v 1.0 - October 2009, Image Creator and program examples.

# Quick Start

- Open Matlab and change the current directory to the directory of the model.
- run `ImageCreator.m`.
- run `ExampleTD.m`.

The first program creates and saves a matrix of sources for a cavity which dimensions match the dimensions of the reverberation chamber (RC) at the IETR. The second program loads the matrix and returns the channel impulse responses, the frequency response and the responses to an arbitrary signal calculated for a given reception point along the three rectangular components.

# Chapter 1

## Understanding the Model

### 1.1 Image Theory

Image theory is generally introduced with electric charges. Let a positive charge be placed at a distance  $d$  from an infinite perfectly conducting plane (Fig. 1.1-(a)). This conductive plane is an anti-symmetrical plane, thus a negative charge is facing the negative charge. The resulting field of the positive charge and the plane is the field created by an electrostatic dipole with the two charges (Fig. 1.1-(b)). Image theory can be applied to moving charges. Fig. 1.2 sums up the different possible configurations with an electric current vector  $\vec{i}$ .

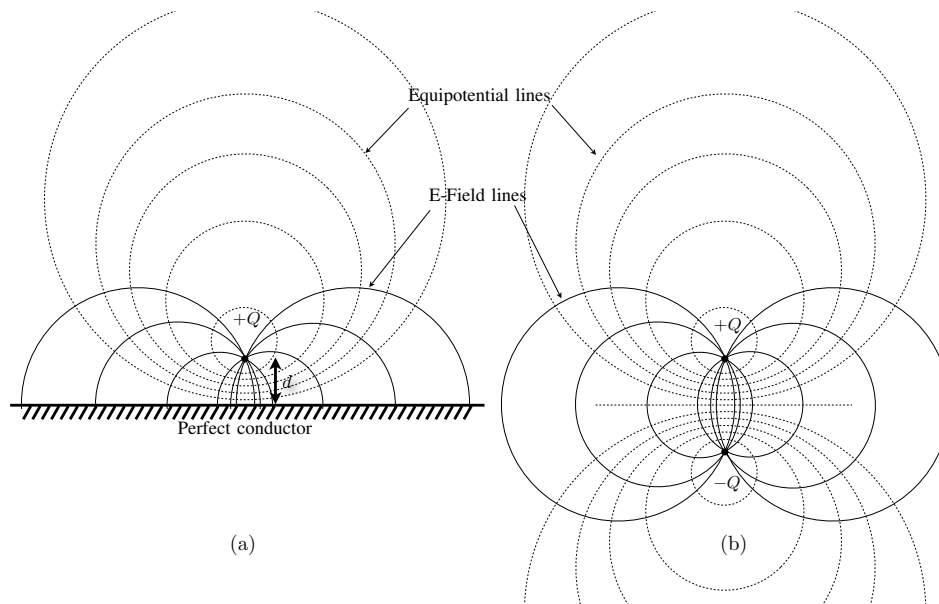


Figure 1.1: Image theory applied to an electric dipole.

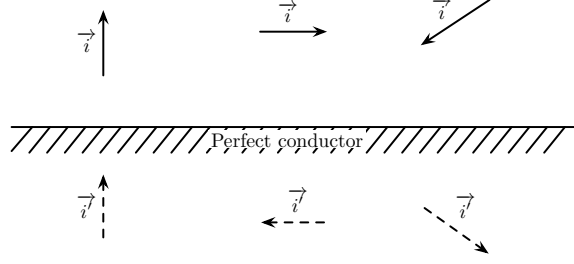


Figure 1.2: Image theory applied to electrical currents.

## 1.2 Image Theory Applied to Cavities

### 1.2.1 Images

Fig. 1.3, inspired by [2], presents a vertical and an horizontal view of the image currents created by applying the construction rules presented in Fig. 1.2 to an arbitrarily oriented current in a rectangular cavity. The real cavity (in bold line, in the middle) is surrounded by image cavities. Each image cavity contains an image current. We define the order of an image current, *i.e* the order of an image cavity, as the number of reflections involved in its creation. The number of cavities for a given order  $n \geq 1$  is given by

$$N_n = 4n^2 + 2 \quad (1.1)$$

and the total number of cavities till the order  $n$  is given by

$$\begin{aligned} M_n &= 1 + \sum_{i=1}^n (4i^2 + 2) \\ &= 1 + 2n + \frac{2n(n+1)(2n+1)}{3}. \end{aligned} \quad (1.2)$$

The growth of  $M_n$  is therefore proportional to  $n^3$ .

### 1.2.2 Cavity Loss

Image theory is applied with perfectly conducting materials. To simulate a lossy rectangular cavity, we introduce three loss coefficients  $R_x$ ,  $R_y$ ,  $R_z$  corresponding to the three pairs of conducting walls of our cavity.<sup>1</sup> In this section we focus on an elementary current  $a$  inside a  $n^{\text{th}}$  order image-cavity. This elementary current is created by  $i$  reflections along the  $Ox$  axis,  $j$  reflections along the  $Oy$  axis, and  $k$  reflections along the  $Oz$  axis. The attenuation associated to this elementary current  $a$  is:

$$R_a = R_x^{|i|} R_y^{|j|} R_z^{|k|}, \text{ with } |i| + |j| + |k| = n. \quad (1.3)$$

The intensity of this current can be written:

$$I_a = I_0 \cdot R_a, \quad (1.4)$$

---

<sup>1</sup>In some situations it can be helpful to have three distinct coefficients to simulate an open door or a lossy wall, in general however, these three coefficients are equal. If you really want to use different coefficients (anisotropic loss), you can use the full losses version of the model.

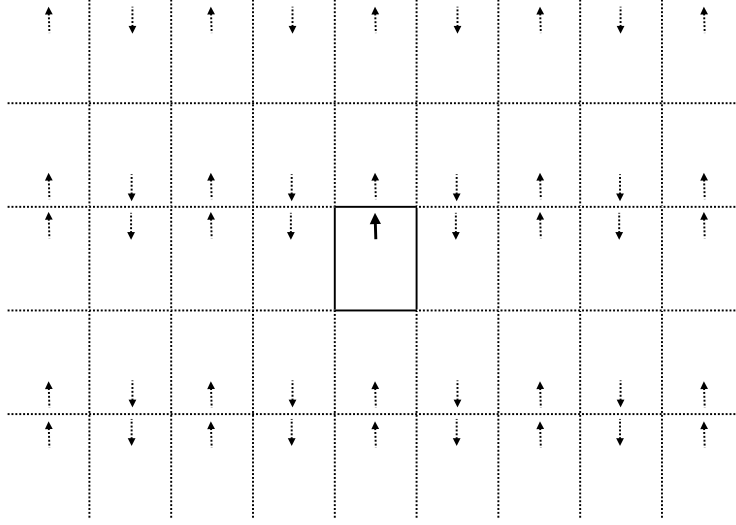


Figure 1.3: Image theory applied to a rectangular cavity.

where  $I_0$  is the intensity of every current in the system if the walls are perfectly conducting. Assuming  $R = R_x = R_y = R_z$ , the total amount of energy  $\mathcal{E}_{tot}$  found in the system is proportional to:

$$\mathcal{E}_{tot} \propto I_0^2 + \sum_{i=1}^{\infty} (4i^2 + 2) I_0^2 \cdot R^{2i}. \quad (1.5)$$

As  $R < 1$ , the sum above converges.

### 1.2.3 Channel Impulse Response Calculation

The intensity of the particular elementary current  $a$ ,  $\vec{I}_a$  can be written:

$$\vec{I}_a = I_a \cdot \vec{w} = I_0 R_x^{|i|} R_y^{|j|} R_z^{|k|} \cdot \vec{w}, \quad (1.6)$$

where  $\vec{w}$  is the normalized vector along the direction of the considered elementary current. The current in the real cavity and all the image currents simultaneously emit an elementary impulse  $f(t)$ . The intensity of the elementary current  $a$  can be written:

$$I_a(t) = I_0 R_a \cdot f(t), \text{ with } f(t) = \begin{cases} 1 & \text{if } t = 0, \\ 0 & \text{otherwise.} \end{cases} \quad (1.7)$$

The orientation of the current at this position is given by a tilt angle  $\alpha$ , defined by the angle between  $\vec{w}$  and  $\vec{e}_z$  and an azimuthal angle  $\beta$  defined by the angle between  $\vec{w} - (\vec{w} \cdot \vec{e}_z) \vec{e}_z$  and  $\vec{e}_x$  (Fig. 1.4). The electrical field created by the elementary current  $a$  and received at a reception point  $P$  within the real cavity can be written<sup>2</sup>:

$$\vec{E}_a(t) = -\omega\mu \frac{dh I_0 R_a f(t - t_a)}{4\pi d_a} \sin \theta_a \begin{cases} \cos \theta_a \cos \phi_a \cdot \vec{u} \\ \cos \theta_a \sin \phi_a \cdot \vec{v} \\ -\sin \theta_a \cdot \vec{w} \end{cases}, \quad (1.8)$$

---

<sup>2</sup>(1.8) is valid for a dipole radiation pattern ( $-\sin \theta$ ). One should note that any 3-D radiation pattern function of  $\theta$  and  $\phi$  can be employed.

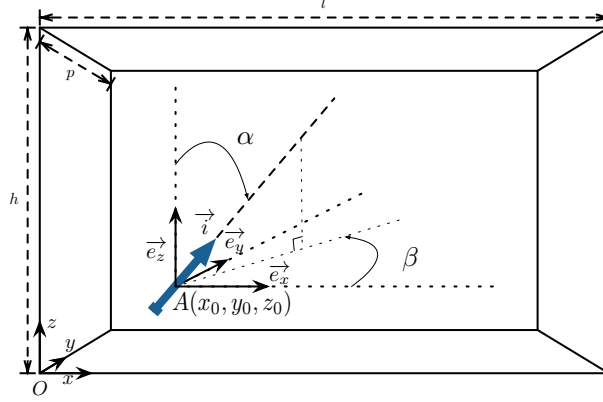


Figure 1.4: Angles and coordinates of the elementary dipole in the cavity.

with

$$\begin{cases} \vec{u} = \mathcal{R}_{\alpha,\beta} \cdot \vec{e}_x \\ \vec{v} = \mathcal{R}_{\alpha,\beta} \cdot \vec{e}_y \\ \vec{w} = \mathcal{R}_{\alpha,\beta} \cdot \vec{e}_z \end{cases} \quad (1.9)$$

where  $dh$  is the length of the elementary dipole,  $d_a$  is the distance between the position of the elementary current  $a$  and the reception point  $P$ ,  $t_a$  is the time of arrival at the reception point, and  $\theta_a$  and  $\phi_a$  are angular coordinates of the point  $P$  in the local spherical coordinate system attached to the elementary current  $a$ .  $\vec{u}$ ,  $\vec{v}$ , and  $\vec{w}$  define the local rectangular basis attached to the elementary current.  $\mathcal{R}_{\alpha,\beta}$  is the rotation matrix<sup>3</sup> that changes the rectangular basis  $(\vec{e}_x, \vec{e}_y, \vec{e}_z)$  into the local basis  $(\vec{u}, \vec{v}, \vec{w})$  and  $c$  is the celerity.

From the E-field expression (1.8) in the local rectangular coordinate system attached to the elementary current, we can deduce the expression in the rectangular coordinate system attached to the simulated cavity:

$$\begin{aligned} \vec{E}_{a(\vec{e}_x, \vec{e}_y, \vec{e}_z)} &= \mathcal{R}_{\alpha,\beta}^{-1} \cdot \vec{E}_{a(\vec{u}, \vec{v}, \vec{w})} \\ &= \mathcal{R}_{-\alpha,\beta} \cdot \vec{E}_{a(\vec{u}, \vec{v}, \vec{w})}. \end{aligned} \quad (1.11)$$

The channel impulse response is given by adding the contribution of every current in our system. If  $M$  is the total number of currents in our system, from (1.8) we can deduce three channel impulse responses corresponding to the three rectangular components:

$$s_{x,y,z}(t) = \sum_{i=0}^M \vec{E}_i(t) \cdot \vec{e}_{x,y,z}. \quad (1.12)$$

The channel impulse response can be convoluted with a chosen signal to simulate the waveform obtained at the position  $P$  in the shielded cavity. By applying a Fourier transform on the channel impulse response, the frequency domain of the cavity can be studied.

<sup>3</sup> $\mathcal{R}_{\alpha,\beta}$  represents a rotation of an angle  $\alpha$  around a unitary vector  $\vec{e}_\beta = -\cos \beta \vec{e}_x + \sin \beta \vec{e}_y$ ,

$$\mathcal{R}_{\alpha,\beta} = \begin{pmatrix} \cos^2 \beta + (1 - \cos^2 \beta) \cos \alpha & -\cos \beta \sin \beta (1 - \cos \alpha) & \sin \beta \sin \alpha \\ -\cos \beta \sin \beta (1 - \cos \alpha) & \sin^2 \beta + (1 - \sin^2 \beta) \cos \alpha & \cos \beta \sin \alpha \\ -\sin \beta \sin \alpha & -\cos \beta \sin \alpha & \cos \alpha \end{pmatrix} \quad (1.10)$$



One should note that the quantity  $C = -\omega\mu\frac{dhI_0}{4\pi}$  equals 1 V in our model. As our model cannot pretend to be deterministic, obtaining absolute values is not necessary<sup>4</sup>. The E-fields are expressed in  $\text{V.m}^{-1}$  but the values are arbitrary.

#### 1.2.4 Assumptions

Using image theory to model a shielded cavity means that we omit the energy diffracted by the wall edges in the cavity. We only consider the energy reflected by the different walls. This optical approach is validated if the dimensions the cavity involved are substantially bigger than the wavelength<sup>5</sup>. In these conditions the geometrical laws of optics can be applied to the image current emissions. This model uses far-field radiation only, near-field radiations are neglected. The radiating current does not have any physical dimension, but this limitation can be easily bypassed by juxtaposing emitting currents to simulate a radiating line or an antenna in the cavity.

---

<sup>4</sup>This explains that the frequency response does not decay when the frequency increases, the equivalent surface of the antenna is constant in our model.

<sup>5</sup>However, results have shown a good adequacy between measurements and simulations even at low frequency.

## Chapter 2

# Image Creator

### 2.1 Usage

Image creator is a standalone program (`ImageCreator.m`) that returns a matrix of images for a given cavity and a given position and orientation of one or more elementary currents within the rectangular cavity. The input parameters are the dimensions of the cavity, the desired time-window of the simulation, and the attributes of every emitting elementary current (position, angular orientation). You may create array antennas by tweaking the positions and adding phase and the amplitude information in the matrix. The matrix `POS` (for position) created by this program contains  $M$  elementary currents, each line describes a current (Tab. 2.1).

x-position		y-position		z-position		$ i  +  j  +  k $		$\alpha$		$\beta$	
------------	--	------------	--	------------	--	-------------------	--	----------	--	---------	--

Table 2.1: Description of a line of the matrix `POS`, corresponding to a  $n^{th}$  order current with  $i$  reflections along the axis  $Ox$ ,  $j$  reflections along the axis  $Oy$  and  $k$  reflections along the axis  $Oz$ .

### 2.2 How to Construct Images When Time is Money

Let a rectangular cavity be of length  $l$ , width  $p$ , and height  $h$ . A corner of this cavity is the origin of the rectangular coordinates and the three main directions  $Ox$ ,  $Oy$ , and  $Oz$  are defined by the edges of the cavity.

Let an elementary current be placed within this cavity at the point  $A(x_0, y_0, z_0)$ , its angular orientation in the cavity is defined by a tilt angle  $\alpha$  and an azimuthal angle  $\beta$  as presented in Fig. 1.4. Generating the elementary image current means that we have to determine the position and the angular orientation of every current created by the reflections with the walls and save the number of reflections involved for each direction. A one-by-one image creation process can take days to generate millions of sources. The first step is to identify patterns in Fig. 2.1 to speed-up the image creation process.

An elementary current can be identified by the reflections involved in its creation. If we consider a  $n^{th}$  order current created by  $i$  reflections along the axis  $Ox$ ,  $j$  reflections along the axis  $Oy$ ,  $k$  reflections along the axis  $Oz$ , we have  $n = |i| + |j| + |k|$ <sup>1</sup>. If we examine the horizontal plane ( $k = 0$ ) represented

---

<sup>1</sup>The numbers  $i$ ,  $j$  and  $k$  can be negative if the reflections are in the decreasing direction along the respective axis.

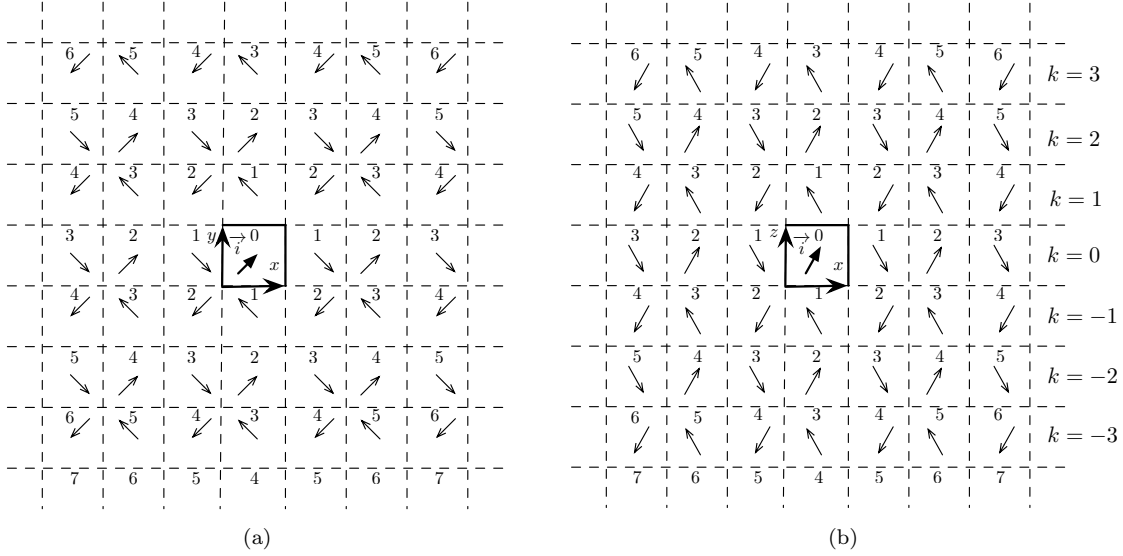


Figure 2.1: Image cavities and image currents in an horizontal plane ( $k = 0$ ) (a) and a vertical plane ( $j = 0$ ) (b). The order of each cavity is indicated.

in Fig. 2.1(a), we can notice that we need to compute one line of sources for example  $j = 0$ ,  $k = 0$  and deduce the line  $j = 1$ . Then a duplication of these two kind of lines give the horizontal plane  $k = 0$ .

In the same manner, if we study the orientations of the elementary currents in a vertical plane (Fig. 2.1(b)), we can discern that the parity of  $k$  dictates the orientation of the current in the corresponding horizontal plane. There are only two different horizontal planes. We already have the plane  $k = 0$  and thus all the even horizontal planes. We can easily derive the odd planes from an even plane, the positions of the currents along the axis  $Ox$  and  $Oy$  are the same and the vertical positions of the elementary currents differ. The height of all the currents in the  $k = 0$  horizontal plane is  $z_0$  and the height of all the currents in the horizontal plane  $k = 1$  is  $2l - z_0$ . The tilt angles are conserved but the azimuthal angles of the currents are reversed. We add  $\pi$  radians to the azimuthal angle of the currents of the plane  $k = 0$  to obtain the azimuthal angles of the currents contained in an odd plane. These two horizontal planes configurations are then duplicated along the  $Oz$  direction, the vertical positions of the generated sources and the number of reflections along the axis  $Oz$  are adjusted accordingly. Creating a full horizontal plane and duplicate it along the vertical direction speeds up considerably the image creation process.

Now we can find 3 planes of symmetry in this system. The planes  $x = 0$ ,  $y = 0$  and  $z = 0$ . It means that the rectangular coordinates can be easily determined by using these three symmetries. Moreover, we only need to generate the images in the space defined by  $x > 0, y > 0, z > 0$  to deduce the positions of all the sources. In order to save memory, we generate only a eighth of the sources and we compute the remaining sources by changing the signs of the rectangular coordinates and by tweaking the tilt and azimuthal angles. These operations that involves basic operations on each column of the POS matrix appear in the program CIR8th.m.

## Chapter 3

# CIR Calculation and More

This chapter is dedicated to the program `ExampleTD.m`. It is a sample program that shows how to get a CIR (through the `CIR` function) a frequency response and an arbitrary signal response for a given cavity and a given position within the cavity.

### 3.1 CIR Computation

The CIR computation is the core of the program. It is assured by the function (`CIR`). The parameters are the three coordinates of the reception point. The loss coefficient (`R`), the position matrix (`POS`), the length of the time-window (`Lt`) become global variables. The function computes a CIR. After loading the position matrix `POS` in the memory, for every image current near enough to appear in the given time-window, the program calculate the position of the reception point in the local coordinate system attached to the image current by using a coordinates transformation matrix. The E-field is then computed in this system of coordinates through an antenna factor named `Antth`. Basically it is the radiation pattern associated to this image current, any 3D radiation pattern as a function of the local angles  $\theta_a$  and  $\phi_a$  can be used. By using the inverse coordinates transformation matrix the E-field is expressed in the usual rectangular coordinates. The contributions of all the image currents are summed and form three CIRs (`Sx`, `Sy`, `Sz`) presented in Fig. 3.1. A vectorized version of the CIR computation will be available soon.

### 3.2 Frequency Response and Response to an Arbitrary Waveform

From the CIRs, we can easily derived a channel frequency response by using a fast Fourier transform. We obtain three frequency responses (`FFTx`, `FFTy`, `FFTz`) presented in Fig. 3.2.

From the CIRs, we can derive the response of the cavity for an arbitrary signal by convoluting the CIRs with a given signal `s`. We obtain three responses (`Signalfinalx`, `Signalfinaly`, `Signalfinalz`) presented in Fig. 3.3.

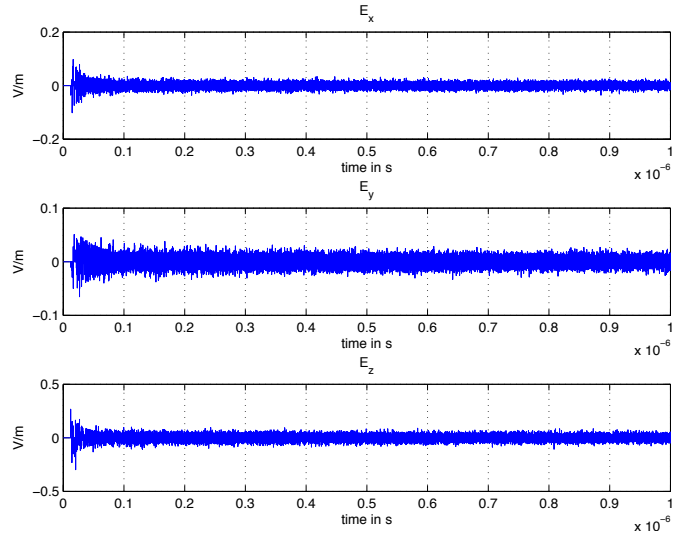


Figure 3.1: Channel impulse responses returned by the program.

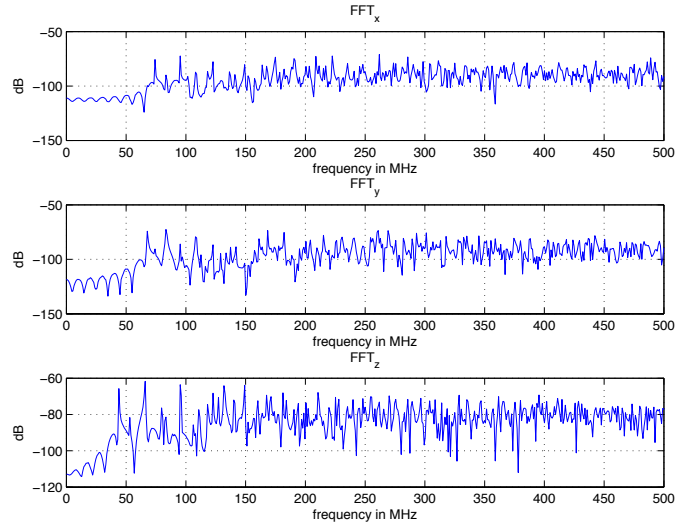


Figure 3.2: Fast Fourier transforms of the CIRs.

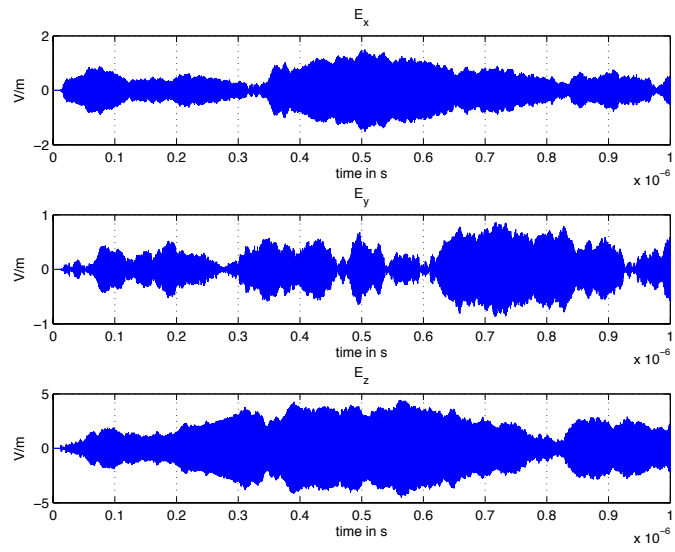


Figure 3.3: Responses to a 300 ns pulse at 1GHz.

## Chapter 4

# Stirring Process

### 4.1 Source Stirring

In our model, there is no mechanical stirring process. However source stirring can be easily achieved by selecting positions of the receiver that produce decorrelated responses. The code below shows how  $M$  decorrelated positions can be chosen in a cavity. We use the criterion that states that positions are decorrelated if the distance between them is superior to  $\lambda/2$  [3]. The routine below generates randomly  $M = 100$  positions for a frequency  $f_0$  and a  $l \times p \times h$  meters cavity:

```
M=100

lambda=c/f0;

X=[(l-lambda)*rand+lambda/2];
Y=[(p-lambda)*rand+lambda/2];
Z=[(h-lambda)*rand+lambda/2];

while (length(X)<M)
    X_1=(l-lambda)*rand+lambda/2;
    Y_1=(p-lambda)*rand+lambda/2;
    Z_1=(h-lambda)*rand+lambda/2;
    D=sqrt((X_1-X).^2+(Y_1-Y).^2+(Z_1-Z).^2);
    if min(D)>lambda/2
        X=[X;X_1];
        Y=[Y;Y_1];
        Z=[Z;Z_1];
    end
end
```

### 4.2 Paddle Simulation

We are currently trying to add a stirring method to our model in order to add a degree of freedom to our simulations. Our first approach would be to simulate an amount of  $M$  situations, in which the position of the emitting elementary dipole is different. By applying the superposition theorem, a stirring step could be a combination of  $N$  simulations among  $M$ . Another approach could be to change the dipole radiation pattern by a more directive pattern and to simulate a paddle with five or six of these directive sources rotating around a chosen axis.

## Chapter 5

# Frequency domain direct calculation

We can compute the frequency response by summing the contribution of every source as an harmonic dipole. This approach allows to introduce frequency dependent loss  $R$  and even volumetric absorption by the water in the air. Use `ExampleFD.m`.

More details soon.



## Chapter 6

# Memory Usage

If the model is relatively straightforward, the memory usage of the algorithm can be a problem. Image-currents are generated numerically and their positions and various attributes<sup>1</sup> are stored in the POS matrix. The number of sources is given by (1.2). In reality the main parameter of the simulation is not the maximum order but the duration of the simulated time-window  $L_t$ . It means that we only need the image-currents within a radius  $c \cdot L_t$ . This filtering can save a lot of memory.

Table 6.1 sums up the memory usage for a given time window. On a 64 bits platform with 32 GB of memory, we manage to reach a time-window of 12  $\mu s$ .

$L_t$	Number of currents simulated $M$	Memory usage
1 $\mu s$	$1.1 \times 10^6$	1 MB
3 $\mu s$	$27 \times 10^6$	213 MB
5 $\mu s$	$119 \times 10^6$	955 MB
10 $\mu s$	$930 \times 10^6$	7.5 GB
100 $\mu s$	$9 \times 10^{11}$	7 TB

Table 6.1: Length of the simulated time-windows and memory usage for the RC at the IETR

The sources are contained in a sphere, their number  $M$  can be roughly obtained by calculating:

$$M \sim \frac{4\pi(cL_t)^3}{3lph}. \quad (6.1)$$

Increasing gradually the time-window in the image creator program can be helpful to determine the maximum time-window allowed by your system. Because 32 bits systems can only address 4 GB of memory, 64 bits systems are strongly recommended to run this program.

We have constantly improved the memory usage of our model, by filtering the images and by using symmetries, we are convinced that it can still be improved. We would be happy to have suggestions and comments about that.

---

<sup>1</sup>For each current the attributes are: the rectangular coordinates, the order, tilt and azimuth angles.

## Chapter 7

# Loss Coefficient Estimation

### 7.1 Measurement approach

The loss coefficient used in our model is empirically determined by using a measurement of the channel impulse response with a given loading. We used the following methodology. First, we measure a channel impulse response. We use an arbitrary waveform generator (Tektronix<sup>®</sup> AWG 7052) to create the shortest impulse possible (200 ps, 2.5 GHz of bandwidth). The antennas used are generally a pair of wide band horn antennas or discone antennas. The signal is averaged to increase the SNR and recorded on a digital storage oscilloscope (Tektronix<sup>®</sup> TDS6124C at 40 GS/s). This signal is then transformed using Matlab<sup>®</sup>. We compute the square of the signal and we make several simulations with different values of  $R$ . In order to compare the simulations with the measurement, both the simulations and the measurement are normalized so that the cumulative power after 3  $\mu$ s equals 1. These simulations are compared with measurements and we identify graphically the correct value of  $R$ . Fig. 7.1 shows how the value of  $R$  is chosen, the idea is to find the value of  $R$  (among 501 values between 0.95 and 1) that fits the most the measurement. In this case the value  $R = 0.9924$  fits the measurement made in our RC with one absorber.

Practically  $R$  values higher than 0.995 are used to simulate an empty cavity. Values under 0.995 are used to simulate a loaded cavity.

If there is too much loading in the chamber to perform a CIR measurement, one can use a long sinusoidal pulse measurement over  $N$  stirrer positions. And then the same situation can be simulated with  $R$  varying from 0.95 to 1 and  $N$  positions of the receiver. The matching  $R$  coefficient can be determined by comparing the averages of the measured and simulated data.

#### 7.1.1 Semi theoretical approach

If we consider that in an RC, the CIR follows an exponential function, the power measured can be written:

$$P_m(t) = P_{m0}e^{-t/\tau}, \quad (7.1)$$

where  $\tau$  is the time constant of the power measured.

In the numerical model, if we consider the  $4i^2 + 2$  currents of order  $i$ , the fraction of the magnitude of the E-field of each source that reaches the initial cavity is approximately  $4\pi/(4i^2 + 2)$ . Therefore, if we make the assumption that the incoming E-field from the  $i^{\text{th}}$  order currents arrives before the E-field

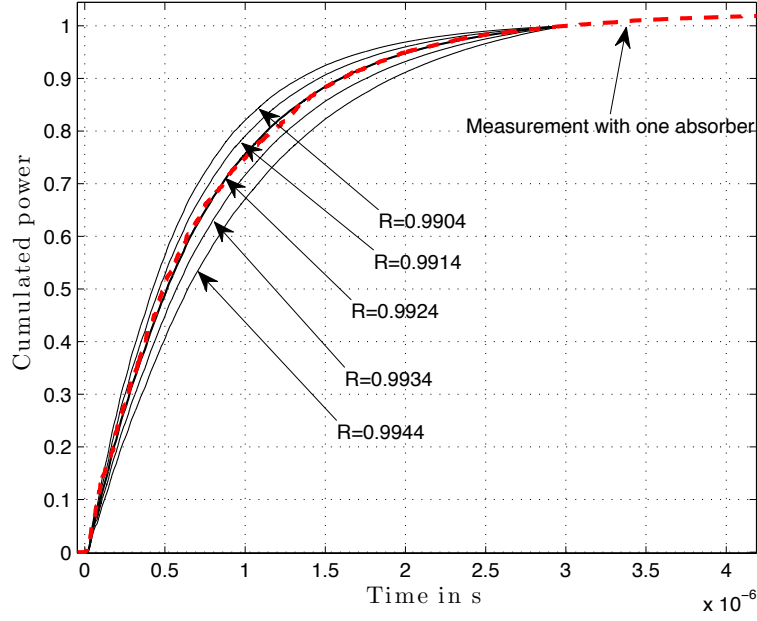


Figure 7.1: Measured cumulated power with one absorber vs. time and simulations with different values of  $R$ . In this case the value  $R = 0.9924$  fits the measurement.

from the the  $(i + 1)^{\text{th}}$  order, we can estimate the E-field from the  $4i^2 + 2$  currents of order  $i$ :

$$E(i) \approx E_0 R^i \quad (7.2)$$

The theory of acoustic reverberation chamber gives the average length of a path between two reflexions on the walls [4].

$$L = \frac{4V}{S}, \quad (7.3)$$

where  $V$  is the volume of the cavity and  $S$  its surface. The E-field from the currents of order  $i$  arrive approximately at the instant  $t = iL/c$ . We can write the power received :

$$P(t) \approx P_0 R^{2t \frac{c}{L}} \approx P_0 e^{2t \frac{c}{L} \ln R}, \quad (7.4)$$

and:

$$\tau \approx -\frac{L}{2c \ln R}. \quad (7.5)$$

From a measurement of  $\tau$  we can derive a value of  $R$ . Therefore, with a given loading in the chamber, we can measure the corresponding time to live  $\tau_m$  and estimate the correct value of  $R$ .

## Chapter 8

# Applications

Here is a non exhaustive list of applications of this model:

- Study the physics of the chamber,
- Waveform simulation [1, 5],
- Transients studies [1, 5],
- Lowest usable frequency determination [1],
- Frequency domain behavior of a given cavity [6],
- Influence of the loading on the frequency-domain and the time-domain behavior [5],
- Time-reversing simulations in an RC,
- Channel simulation,
- ...

# Bibliography

- [1] E. Amador, C. Lemoine, P. Besnier, and A. Laisné, “Reverberation chamber modeling based on image theory: Investigation in the pulse regime,” *Electromagnetic Compatibility, IEEE Transactions on*, vol. 52, no. 4, pp. 778 – 789, 2010.
- [2] R. Harrington, *Time-Harmonic Electromagnetic Fields*. New York: McGraw-Hill Book Company, 1961.
- [3] D. Hill and J. Ladbury, “Spatial-correlation functions of fields and energy density in a reverberation chamber,” *Electromagnetic Compatibility, IEEE Transactions on*, vol. 44, no. 1, pp. 95–101, Feb 2002.
- [4] T. Rossing, Ed., *Handbook of Acoustics*. New York: Springer-Verlag, 2007, ch. 6, pp. 207 – 238.
- [5] E. Amador, C. Lemoine, P. Besnier, and A. Laisné, “Studying the pulse regime in a reverberation chamber with a model based on image theory,” *Proceedings of IEEE International Symposium on EMC, Fort Lauderdale, Florida, U.S.A.*, 2010.
- [6] —, “Fine analysis of the behavior of a reverberation chamber in the frequency domain with a model based upon image theory,” *Proceedings of EMC Europe 2010, Wroclaw, Poland*, 2010.